STATIC BEHAVIOR OF CHS-TO-RHS K/KK-JOINTS WITH WELDED SECTION CHORD

SHUANG QIU[1], XIANZHONG ZHAO[1*], SHANSHAN HAN[1], and YIYI CHEN[1]

[1] *College of Civil Engineering, Tongji University, Shanghai 200092, China.*
E-mail: x.zhao@tongji.edu.cn

Tubular joints with RHS (Rectangular Hollow Section) chord fabricated by welding four plates together is commonly seen in China due to its flexible section dimensions. There are, though, some uncertainties in the safe application of the design formulae for CHS-to-RHS joints with welded chord section, due to the lack of sufficient experimental study. This paper presents the experimental investigation on four CHS-to-RHS K/KK-joints with RHS chords made of welded section and another two K/KK-joints with cold-formed chords. The static behavior of the joints, including failure mode and ultimate capacity were studied. Experimental results show obvious difference in failure mode between welded chord and cold-formed chord, where corner weld cracking is the main failure mode for the former while chord plastification governs the failure of the latter. For the joints with welded section, the poor post-peak behaviors were observed. The final failure modes also showed that fabrication quality of chord sections played an important role in the joint static behavior. Even though the peak load obtained from the tests satisfied the design capacity specified by general design guides, the welded chord section with uncertain welding quality should be strictly avoided in joints with high β (ratio of brace diameter to chord width) and those used with high seismic requirements due to brittle failure.

Keywords: CHS-to-RHS K/KK-joint, welded hollow section, static behavior, failure mode, ultimate capacity.

1 Introduction

Owing to easier fabrication for requiring no complex intersection line cutting, RHS (Rectangular Hollow Section) chord is sometimes used as an alternative of CHS (Circular Hollow Section) chord. Therefore, CHS-to-RHS joint, the tubular joint with the CHS braces directly welded to the RHS chord, is sometimes used in tubular structures. General design guides on tubular joins with RHS chord are applicable to both hot-finished and cold-formed steel hollow section (Packer 2009). However, RHS chord fabricated by welding four plates together is more commonly used in practical construction in China due to its flexible section dimensions. However, due to the lack of sufficient experimental study, there are uncertainties in the safe application of the design formulae for the CHS-to-RHS joints with welded section chord.

As CHS-to-RHS joints show similar mechanical behaviors as that of RHS-to-RHS joints (Packer 1978, Wardenier 1979), the current capacity formulae of CHS-to-RHS joint are based on the formulae for RHS-to-RHS joint, in which the brace width b is replaced by the brace diameter d, and additional brace conversion factor of $\pi/4$ is multiplied. As for multi-planar KK-joint, the factor of 1.0 is recommended by CIDECT, which means the multi-planar effect is ignored for KK-joint. The conclusions above were both drawn by a series of experiments of

Proceedings of the 17th International Symposium on Tubular Structures.
Editors: X.D. Qian and Y.S. Choo

Published by Research Publishing, Singapore.
ISBN: 978-981-11-0745-0; doi:10.3850/978-981-11-0745-0_119-cd

joints with cold-formed or hot-finished members. While for the joint with welded section chord, the results might be different due to the different mechanical mechanism and failure mode.

In this paper, the static behavior of CHS-to-RHS K/KK-joint with welded section chord was studied. The experimental investigation includes four joints with welded section and two joints with cold-formed section for the sake of comparison. Obvious differences were shown in the behaviors of cold-formed chord and welded chord. Based on the experimental results, the effects of chord section type, geometrical parameter and multi-planar braces were studied. The recommendations for welded section members used in tubular joints are given according to the results.

2 Experiment Program

Six specimens, including two K-joints with welded section chords and four KK-joints with cold-formed and welded section chords, were tested. The welded section of the chord was composed of four plates joined by partial penetration weld. The RHS chords in this paper are all square section with nominal dimension of 280×10 (mm, height/width × thickness). Figure 1 shows the configuration of CHS-to-RHS joint specimens, including the side view of K-joint and KK-joint. The figure also shows the constant geometric dimensions and parameters used in the test: the eccentricity of two brace intersection e_0 and inclined angle of brace θ in K-plane were 50mm and 45°, and the nominal parameters γ (ratio of chord width to twice thickness) and τ (ratio of brace to chord thickness) were 14 and 0.8, respectively. Other varied parameters were listed in Table 1. The specimens were labelled as Joint Type (K- or KK-joint) – Chord Section Type (Welded, identified as W or Cold-formed, identified as C) – Brace Diameter (133 or 219), as shown in Table 1.

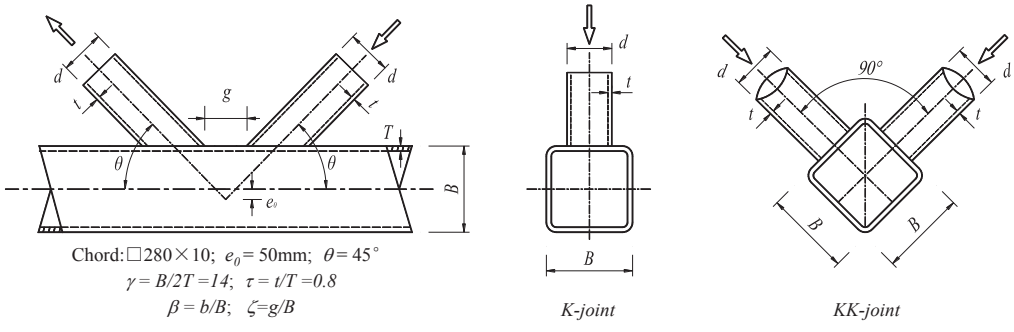

Figure 1. CHS-to-RHS K/KK-joint: Geometric dimensions and parameters

Table 1. Specimens and varied parameters

Labels	Joint Type	Brace Dimensions (mm, d×t)	β (b/B)	ζ (g/B)	Chord Section Type
K-W-133	K-joint	ϕ133×8	0.475	0.685	Welded
KK-W-133	KK-joint	ϕ133×8	0.475	0.685	Welded
K-C-219	K-joint	ϕ219×8	0.782	0.251	Cold-formed
K-W-219	K-joint	ϕ219×8	0.782	0.251	Welded
KK-C-219	KK-joint	ϕ219×8	0.782	0.251	Cold-formed
KK-W-219	KK-joint	ϕ219×8	0.782	0.251	Welded

The two braces in the K-plane were subjected to simultaneous and equal-magnitude compressive and tensile loadings, respectively, through hydraulic actuators. As for KK-joint, the braces were symmetrically loaded in the two K-planes. The experiments were carried out in the multi-functional spherical reaction frame to meet the multi-planar loading demand (Zhao 2019). In the test assembly, the chord was mounted with one end fixed and the other end sliding supported, and the two or four braces were in simply contact with loading actuators, making no moment transferred to the braces. The chords of specimens were long enough to eliminate the effect of boundary restraint (Lee 1995). The displacement transducers (LVDT), as well as strain gauges and strain rosettes, were located at the joint zone to monitor the deformation and strain distribution during the test.

Three tensile test coupons were extracted from each tube member. Considering the effect of cold forming on mechanical properties, the coupons were extracted both from plate and corner of cold-formed chord. The material properties of members were averaged and listed in Table 2, together with the measured wall thickness of each member.

Table 2. Material properties of members

Member	Yield Strength (N/mm^2)	Tensile Strength (N/mm^2)	Elongation (%)	Measured Thickness (mm)
ϕ133×8	412	590	29.95	8.30
ϕ219×8	381	579	32.03	8.32
Welded Chord	363	604	39.52	9.87
Cold-formed Chord (Plate)	389	690	46.25	9.66
Cold-formed Chord (Corner)	578	686	24.82	9.66

3 Experimental Results

3.1 *Experimental observations and failure mode*

Deformation limit of 3% chord width (0.03B=8.40mm) (Lu 1994) was used to measure the joint capacity. Specimens were loaded monotonically until the final failure. Figure 2 shows the final failure modes for different specimens with details described below:

For specimen K-W-133: during the test, the strain rosettes at the crown point of compressive brace indicated that yielding started under the brace load of 310kN. The brace load kept rising as the chord face plastification developing gradually, and the load reached 539kN at deformation limit. At the peak load of 1026kN, the chord face of the tensile brace failed by punching shear suddenly, as shown in Figure 2(a).

Specimen KK-W-133: the crown point of one tension brace started to yield at a load of 292kN. Before reaching the deformation limit, the chord corner near the two tension braces cracked suddenly and the load reached the first peak at 438kN and then fell to 390kN. The weld cracking at the corner propagated along the chord as the load increased, and the second peak load stopped at 568kN, as shown in Figure 2(b).

Specimen K-C-219 & KK-C-219: Similar to K-W-133, the combined failure of chord plastification and punching shear of tensile brace was shown in the two specimens of cold-formed chord, as indicated by Figure 2(c) & (e). For both specimens, the yielding on the chord surface was first observed at the saddle point of the tensile brace near the corner. The yielding-observed load, the load at deformation limit and the peak load are 861kN, 1258kN, 1574kN for the K-joint specimen and 669kN, 1323kN, 1358kN for the KK-joint specimen.

Specimen K-W-219 & KK-W-219: The corner weld cracking at two sides of K-plane is the final fail mode for both the two specimens, as shown in Figure 2(d) & (f). During the loading, the peak loads of both two specimens came before deformation limit. Yielding started near the crown point of the tensile brace at 585kN for the K-joint, while at the saddle point near the chord corner of compressive brace at 330kN for the KK-joint. The peak loads of the K- and KK-joint were 1033kN and 1041kN, respectively.

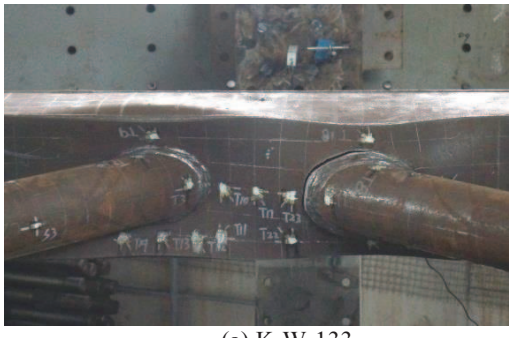

(a) K-W-133

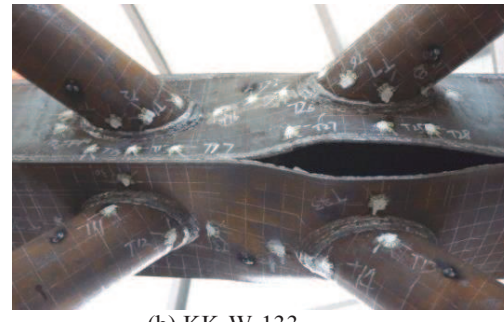

(b) KK-W-133

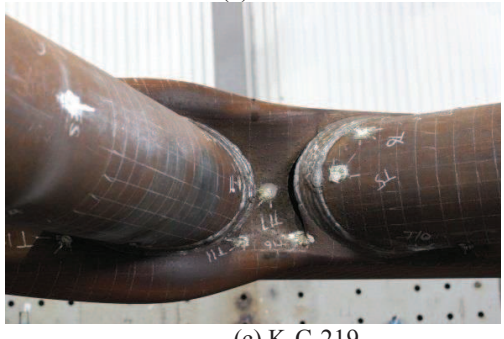

(c) K-C-219

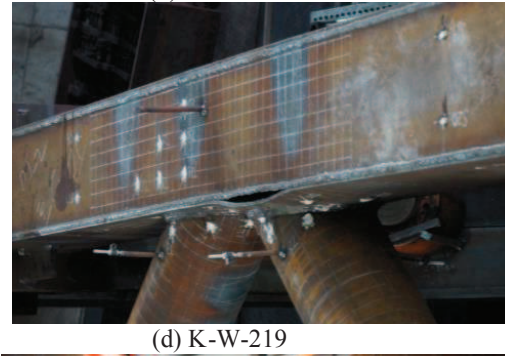

(d) K-W-219

(e) KK-C-219

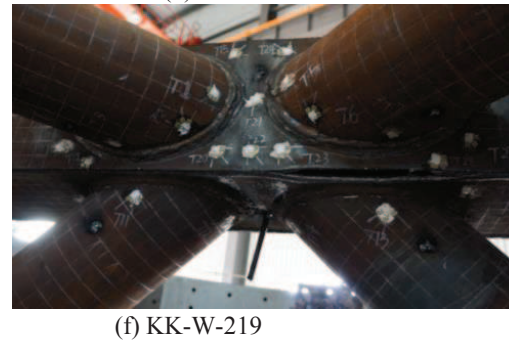

(f) KK-W-219

Figure 2. Final failure modes

3.2 *Load - displacement curves*

Figure 3 & 4 present the axial load-displacement curves for the tensile and compressive brace. The curves were separated by the β ratio for comparison. In these figures, compression curves are given as negative values while tension as positive values. The brace load and displacement were obtained from the cell in servo-controlled actuators, and the brace displacement of KK-joint in the figure was the average of two tensile/compressive braces. The deformation limit (=8.40mm) was marked with the vertical dashed line in all figures.

Figure 3 shows the load-displacement relationships of K/KK-joints with welded chord and ϕ133 brace (small β=0.475). It can be seen that the post-yielding behaviors for the two joints were totally different, and the significant reduction in peak load and ductility of the tensile brace was due to early cracking occurred at the corner of the KK-joint. Figure 4 shows the comparison of the curves of K/KK-joints with ϕ219 brace (large β=0.475). The tensile brace behaviors of K/KK-C-219 were interfered by the adjacent compressive brace due to chord surface plastification, which resulted in the decreased displacement at the late stage of loading. It can be seen that, compared with cold-formed chord, the welded section led to poor joint performance after yielding, especially for the compressive braces. The premature cracks at the chord corner weakened the deformability of the compressive braces, but improved the deformability of tensile braces due to no punching shear failure. The initial stiffness of KK-joint was also weakened due to the welded section chord.

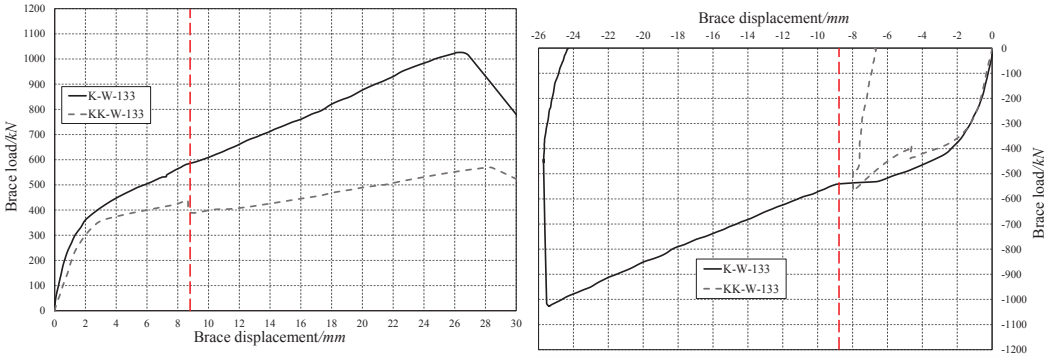

(a) Tensile braces (b) Compressive braces

Figure 3. Brace axial load - displacement curves of joints with ϕ133 brace

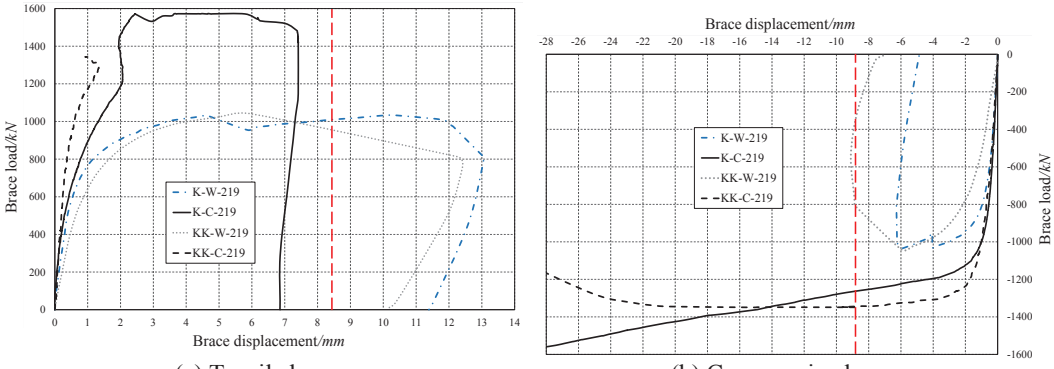

(a) Tensile braces (b) Compressive braces

Figure 4. Brace axial load - displacement curves of joints with ϕ219 brace

3.3 *Ultimate capacity and comparison with design guides*

The ultimate capacity of the joint specimens was determined as the peak load or the load at the deformation limit whichever comes first. Experimental ultimate capacity was given in Table 3. According to the formulae in CIDECT design guide and Chinese code CECS290, the chord face plastification was the governing failure mode, and the predicted capacities, which were based on the measured parameters, were also listed for comparison. It should be noted that the strength

reduction factor of 0.9 is included in CIDECT formulae, while a reduction factor of 0.8 was included in CECS290 to consider the multi-planar effect of CHS-to-RHS KK-joint.

The ratios of experimental to predicted capacity were also given in Table 3. Except the specimen KK-W-133 compared with CIDECT prediction, the results from tests were close to the predicted capacity, or both design code/guide gave rather conservative predicted capacity on the joint with higher β.

Table 3. Comparison of ultimate capacity

Labels	Experimental Capacity (kN)	CIDECT (kN)	Tested-to-Predicted Ratio	CECS290 (kN)	Tested-to-Predicted Ratio
K-W-133	539	519	1.04	558	0.97
KK-W-133	438	519	0.84	447	0.98
K-C-219	1258	854	1.47	944	1.33
K-W-219	1033	854	1.21	944	1.09
KK-C-219	1323	854	1.55	755	1.75
KK-W-219	1041	854	1.22	755	1.38

4 Discussion of Results

4.1 *Effect of chord section type*

It can be seen from Table 3that the welded chord indicated a capacity reduction of 18% for K-W-219 and 21% for KK-W-219 compared with specimen K- & KK-C-219. Different from the common failure, the corner weld cracking is the governing failure mode for the welded chord. The welding residual stress, partial penetration welding condition and significant stress concentration near the tensile brace, as shown by numerical simulation in Figure 5, may be the reasons causing the premature cracking before sufficient plasticity is allowed to develop within the joint zone. For this reason, special attention should be paid to the welding quality of welded RHS members.

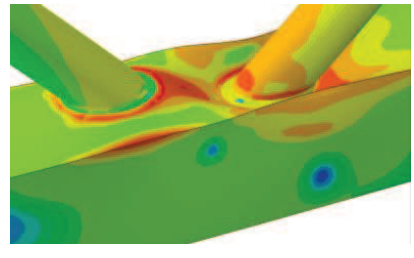

Figure 5. Stress concentration at the non-filleted corner of welded chord

4.2 *Effect of brace diameter (β)*

Failure mode in section 3.1 shows that the chord made of welded section tend to fail in corner weld, while the final failure mode of specimen K-W-133 was a combined surface plastification and punching shear. Compared to K-W-219, the joint with small brace (β=0.475) would endure more sufficient plasticity development within the chord surface, and thus failed in ductile mode. As CIDECT design guide indicates, the joint with higher β would have higher capacity in chord surface. However, the failure load of corner weld would not depend mainly on the brace diameter. It can be inferred from the test that, for joints with welded section chord, as the parameter β increases, the failure mode would shift from chord surface plastification into corner

weld cracking, which is brittle and should be avoided in practice. Thus, for safe application in practice, the β of the joint with welded chord should be strictly limited. In the tests presented in this paper, the β under 0.5 is acceptable for the welded chord with 280×10 (mm) dimension.

4.3 *Multi-planar effect*

The multi-planar effects on the three pairs of K/KK-joint were essentially different. The experimental capacity ratios of KK- to K-joint are 0.82, 1.01 and 1.05 for the pairs of W-133, W-219 and C-219, respectively. For specimen K- & KK-W-133, the multi-planar effect converted the failure mode from chord surface plastification to corner weld cracking, which then led to the significant reduction in both the joint capacity and ductility, as shown in Figure3(b). For specimen K- & KK-W-219, whose failure modes were both cracking at the chord corner, the joint behavior would mainly depend on the corner weld mechanical properties, so the joint behaviors of two specimens, including the brace load-displacement curves, ultimate capacity and strain distribution on the chord surface, were rather close, as shown in Figure 4. The multi-planar effect was marginal.

As for specimen KK-C-219, the side wall deformation of one K-plane was restrained by the other K-plane, so the two planes inter-restrain effect even leads to higher stiffness and lower strain among the joint zone, and thus higher capacity. As a result, the capacity reduction due to multi-planar effect in CHS-to-RHS KK-joint with cold-formed chord can be ignored. Similar conclusions for RHS-to-RHS KK-joint were given by Liu and Wardenier (2001, 2002 & 2003). Based on those, the 2nd edition CIDECT design guide (2009) replaced the previous 0.9 with 1.0 as the multi-planar correction factor.

However, as explained above, the multi-planar effect on the low β joint with welded chord would convert the ductile plastification failure into brittle chord corner cracking. The experimental results indicated about 20% reduction in capacity. The multi-planar correction factor of 0.8 for CHS-to-RHS KK-joint in CECS 290 gave a sound factor for welded chord. For safe application, the welded RHS chord shall be used with more cautions in multi-planar joints with lower β, and should not be used in structures with high seismic requirements because of its brittle failure.

5 Conclusions and Recommendations

Based on the experimental results of six CHS-to-RHS K/KK-joints, the static behavior of joint with welded chord was studied and presented in this paper. The effects of chord section type, brace diameter and multi-plane on joint behavior were investigated. Results show a poor post-peak behavior of joint with welded chord, due to the governing corner welding cracking failure mode. Compared to the cold-formed section, welded chord caused a reduction of about 20% in joint capacity. Different from cold-formed section, the multi-planar effect on the KK-joint with welded chord cannot be ignored due to the alternation of failure mode. According to the experimental results, the welded chord section with uncertain welding quality should be avoided in joints with high β and multi-planar joints, as well as those joints used with high seismic requirements due to their brittle welding cracking failure.

References

CECS 290:2010, *Technical Specification for Structures with Steel Hollow Sections*, China Planning Press, Beijing, China, 2010.

Lu, L.H., deWinkel, G.D. & Yu, Y., Deformation Limit for the Ultimate Strength of Hollow Section Joints, in *6th International Symposium on Tubular Structures*, 341–347, 1994.

Lee, M.M.K. & Wilmshurst, S.R., Numerical Modeling of CHS Joints with Multiplanar Double Configuration, *J. Constr. Steel Res.*, 32, 281–301, 1995.

Liu, D.K., & Wardenier, J., Multiplanar Influence on the Strength of RHS Multiplanar Gap KK-Joints, *Tubular Structures IX*, Swets & Zeitlinger, Lisse, The Netherlands, 203-212, 2001.

Liu, D.K., & Wardenier, J., The Strength of Multiplanar Overlap KK-joints of Rectangular Hollow Sections under Axial Loading, in *Proceedings 12th International Offshore and Polar Engineering Conference*, Kitakyushu, Japan, 34-40, 2002.

Liu, D.K., & Wardenier, J., The Strength of Multiplanar KK-Joints of Square Hollow Sections, in *Proceedings 10th International Symposium on Tubular Structures*, 197-205, 2003.

Packer, J.A., Wardenier, J., Zhao, X.L., van der Vegte, G.J. & Kurobane, Y., *Design Guide for Rectangular Hollow Section (RHS) Joints under Predominantly Static Loading*, CIDECT Design Guide 2nd ed., Geneva, Switzerland, 2009.

Packer, J.A., A Theoretical Analysis of Welded Steel Joints in Rectangular Hollow Sections, Ph.D thesis, University of Nottingham, UK, 1978.

Wardenier, J., *Test on Welded Joints in Complete Girders Made of Square Hollow Sections*, CIDECT Report 5Q-79/5, 1979.

Zhao, X.Z., Qiu, S., Hu, K.H., et al., Capacity of Multi-Planar Out-of-Plane Overlapped Tubular KK-Joints Having Different Joint Details, *J. Constr. Steel Res.*, 158, 182-200, 2019.